Dynamic Channel Model with Overhead Line Poles for High-Speed Railway Communications

Lai Zhou, Zhi Yang, Fengyu Luan, Andreas F. Molisch, *Fellow, IEEE,*
Fredrik Tufvesson, *Fellow, IEEE,* and Shidong Zhou, *Member, IEEE*

***Abstract*—In order to develop reliable communications links for high speed railway (HSR) systems, accurate models for the propagation channel are required. The radio channel properties in HSR scenarios are different from those in cellular scenarios not only due to the high velocity, but also due to the special construction elements and the type of surroundings along the train lines. This paper focuses on the influence of overhead line poles along the railway on the HSR communication channel. The overhead line poles affect the line-of-sight (LOS) communication path periodically, and also act as static and periodic scatterers along railway lines. We performed a measurement campaign at a carrier frequency of 2.4 GHz on the Guangzhou-Shenzhen dedicated high-speed train line in China. Based on the measurement result we propose a dynamic channel model considering periodic poles for HSR communication.**

***Index Terms*—High speed railway, channel measurement, overhead line pole, line-of-sight, channel model.**

I. Introduction

The advance of high-speed railway (HSR) communication has already attracted a lot of attention from both the research community and the industry. The wireless communication link is a critical but challenging element in HSR development. To understand the real radio propagation features, many channel measurement campaigns have been performed in specific scenarios to study channel properties and non-stationary characteristics [1] [2].

In order to model correlation and changing environments, previous works on channel models for HSR mainly focused on geometry-based stochastic channel models (GSCMs) [1] [3], but the developed models do not consider special construction elements like overhead line poles along the railway, that affect the large scale parameters and instantaneous link behavior.

Manuscript received June 28, 2017; revised November 21, 2017; accepted March 18, 2018. This work was supported by the National S&T Major Project (2017ZX03001011), China's 863 Project (2015AA016202), National Natural Science Foundation of China (61631013), Foundation for Innovative Research Groups of the National Natural Science Foundation of China (61621091), Tsinghua-Qualcomm Joint Project, Future Mobile Communication Network Infrastructure Virtualization and Cloud Platform (2016ZH02-3). The work of A. Molisch was supported by the National Science Foundation. Lai Zhou is with the Key Laboratory of Particle and Radiation Imaging (Tsinghua University), Department of Engineering Physics, Tsinghua University, Beijing, China (e-mail: zhoulai13@mails.tsinghua.edu.cn). Zhi Yang, Fengyu Luan and Shidong Zhou are with the Department of Electronic Engineering, Tsinghua University, Beijing, China (e-mail: zhi-yang11@mails.tsinghua.edu.cn; luanfy1987@gmail.com; zhousd@mail.tsinghua.edu.cn). Andreas F. Molisch is with the Department of Electrical Engineering, University of Southern California, USA (e-mail: molisch@usc.edu). Fredrik Tufvesson is with the Department of Electrical and Information Technology, Lund University, Lund, Sweden (e-mail: fredrik.tufvesson@eit.lth.se).

TABLE I
Measurement parameters

Parameter	Setting
Bandwidth	40 MHz
TX height	30 m
RX height	1.2 m
Test signal length	12.8 μs
Moving speed	about 300 km/h

There are some previous studies paying attention to the effect of poles, in example [4] the scattering from traffic signs (cylindrical or rectangular poles) beside the road in vehicular communication scenarios was studied, and in [5] the effect of telegraph poles and electrical wires on the safe distance of a helicopter was studied. The influence of overhead line poles on the wireless propagation is clearly observed in our measurements, and it is advisable to consider such poles in channel modeling. Hence, this paper proposes a dynamic model with periodic poles for HSR communication based on these measurements.

The rest of this paper is organized as follows. A brief introduction of measurement campaign and effect of overhead line poles is described in section II. In section III, we present the measurement results and details of the dynamic model. The model outline with measurement parameters and simulation results are shown in section IV, and at last section V concludes the work.

II. Measurement Campaigns

A. Measurement setup

A wideband channel sounder with center frequency of 2.4 GHz was used to conduct channel measurement on the Guangzhou-Shenzhen dedicated high-speed train line in China [6]. The transmitter (TX) equipped with a directional antenna was mounted on the base station (BS) tower located at the side of the rails; the receiver (RX) equipped with vertically polarized and omnidirectional antenna was fixed on the window of the carriage facing the BS. Details about the measurement configuration are given in Table I.

B. Construction environment along the rail

The special construction elements used for HSRs give rise to specific properties of the propagation environment that are

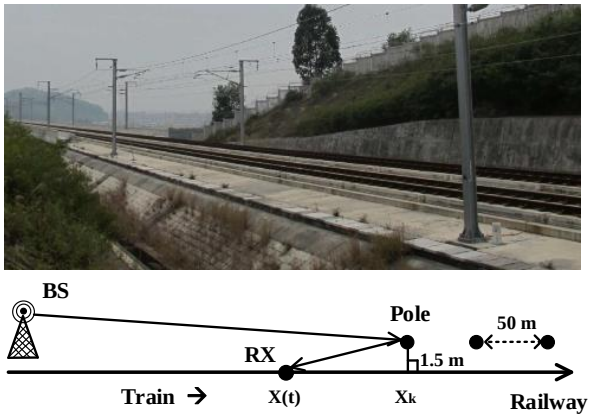

Fig. 1. The overhead line poles along the rail.

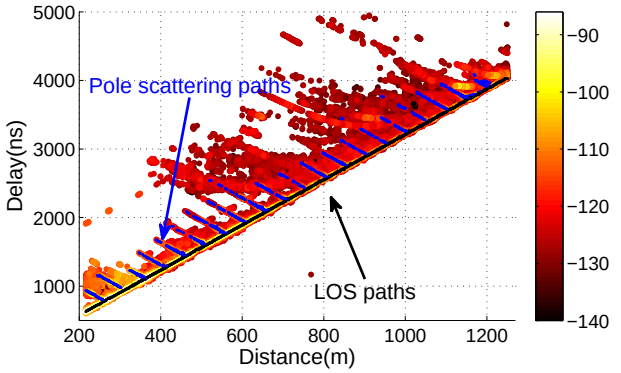

Fig. 2. The distance-delay-power profile of the measured HSR channel.

quite common in a large number of HSR lines in China. A typical scenario in the Guangzhou-Shenzhen dedicated high-speed train line is shown in Fig. 1, including the geometric description of the channel environment. The overhead line poles are spaced 50 m apart to provide electricity along the rail, and the nearest distance between the pole and the RX is less than 1.5 m [6]. The TX mounted on the BS tower is high and close to the track, so the LOS path typically dominates the channel impulse response. The overhead line poles act as both obstructions of the LOS path and as major static scatterers.

III. Measurement Result

The Subspace Alternating Generalized Expectation-maximization (SAGE) algorithm [7] is used to obtain estimates of the multipath propagation components (MPCs) from the measurements, and a geometrical cluster-based scatterer detection method [8] is used to classify different kinds of paths. In order to study the influence of poles, we only analyze the LOS subset and pole scattering (PS) subset of the MPCs as given by the classifier. Fig. 2 shows the two kinds of classified MPCs in the distance-delay-power profile, LOS paths are the black lines with shortest delay for each measurement distance, and PS paths are the blue lines, which are caused by the poles along the rail.

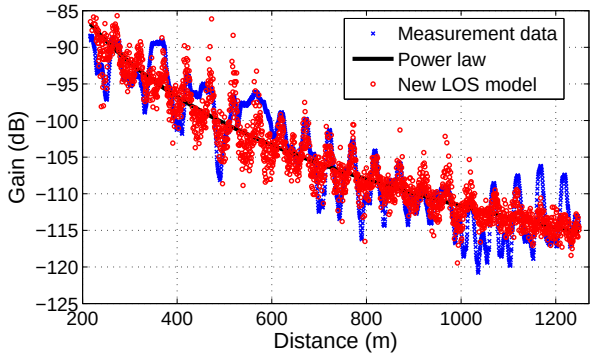

Fig. 3. The LOS path gain along the rail.

A. LOS path Amplitude

Fig. 3 shows that the amplitude of the LOS path can be seen as a distance-decaying part with the addition of a fading, while the fading varies periodically along the distance, which can be modeled with its first and second order harmonic components. Compared to the conventional power law, a new LOS model with periodic fading is proposed as below,

$$A_L(t) = A_{ref,L} - 10n_L \log_{10}\left(d(t)/d_{ref,L}\right) + S_L(d(t)), \quad (1)$$

$$\begin{aligned} S_L(d(t)) =& a_1(d(t)) + a_2(d(t)) \cdot sin(\omega d(t) + \Psi_2) \\ &+ a_3(d(t)) \cdot sin(2\omega d(t) + \Psi_3), \end{aligned} \quad (2)$$

where $d(t)$ is the propagation distance of the LOS path at time t, $A_{ref,L}$ is the power gain at a reference distance $d_{ref,L}$, n_L is the path loss exponent, $S_L(d(t))$ is the large scale fading, where a_i has a lognormal distribution with variance $\sigma^2_{L,i}$, a_1 relates to the static part of fading, a_2 and a_3 relate to the periodic part of the fading, ω is the fluctuation frequency of the LOS obstruction, and Ψ_i is the phase offset.

Fig. 3 shows the measured LOS path gain variation with different distances between TX and RX. The black curve is based on a conventional power law with $S_L(d(t))$ equating 0. The red dotted-line is obtained by the new LOS model (2). It can be clearly seen that the most samples generated by the new periodic fading model match well with measurement data.

In the new LOS model, the large scale fading $S_L(d(t))$ is divided into three independent fading processes with correlated characteristics based on physical fading sources. The first fading part is from, e.g., surrounding trees and buildings. As for the periodic parameters ω in part two and part three, the estimated parameter is $\omega = 2\pi \times 0.02\ rad/m$. Since the distance d_{p-p} between adjacent poles is 50 m, the value of the periodic parameter corresponds to

$$\omega = \frac{2\pi}{d_{p-p}}, \quad (3)$$

representing the periodic fading characteristics of the poles. The value of Ψ_i is in general uniformly distributed between 0 and 2π, but is in Fig. 3 optimized to achieve a good fit with the measured data, resulting in $\Psi_2 = 5.40\ rad$, $\Psi_3 = 2.76\ rad$. The distance dependent autocorrelation function of each part could be calculated as

$$r_i(\Delta d) = E[a_i(d)a_i(d + \Delta d)], \quad (4)$$

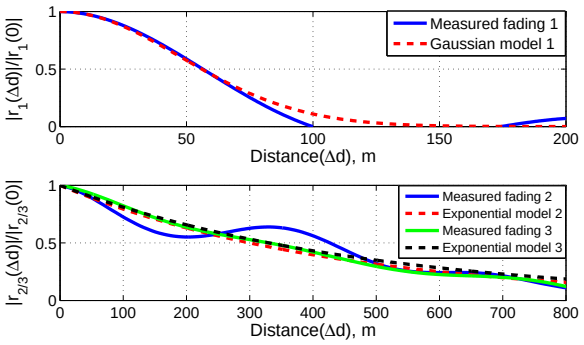

Fig. 4. Distance based autocorrelation for the different fading components in (2).

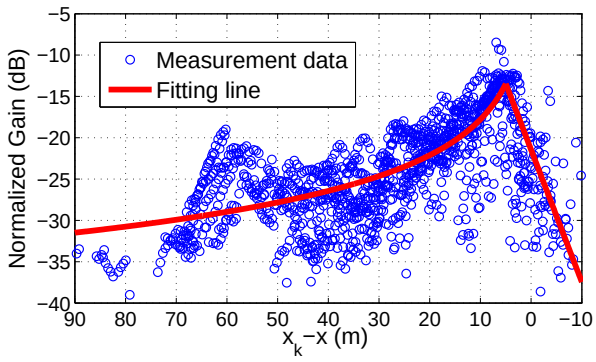

Fig. 5. The scattering path gain from the pole.

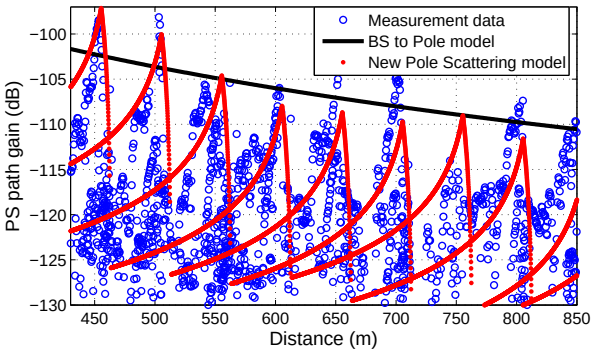

Fig. 6. The PS path gain along the rail.

where Δd is the distance between two positions. There are two functions often used in the literature to describe the auto-correlation function $r_i(\Delta d)$, function (5) assumes a Gaussian decay [9], and function (6) used in 802.16J [10] assumes an exponential decay. We choose the better function for each part based on our data analysis as

$$r_{L,i}(\Delta d) = \begin{cases} \sigma_{S,i}^2 e^{-\frac{\ln 2}{d_{L,i}^2}(\Delta d)^2}, i = 1, & (5) \\ \sigma_{S,i}^2 e^{-\frac{\ln 2}{d_{L,i}}(\Delta d)}, i = \{2,3\}, & (6) \end{cases}$$

where $d_{L,i}$ is the de-correlation distance. Fig. 4 shows the empirical autocorrelation function of the different independent fading components in (2) together with the best fit models.

B. Pole Scattering Amplitude

The PS model consists of two parts, the path loss from BS to the pole (B2P) and the path loss from pole to receiver (P2R). The propagation between the BS and the pole can be modeled as LOS since the BS can almost always "see" the poles, while the P2R part models the scattering mechanism. The PS model is expressed as

$$A_{P,k}(t) = G_k + A_{P,0}(d_k(t)), \quad (7)$$

where $A_{P,k}(t)$ is the power gain of the signal from the k^{th} pole, G_k is the decay factor of the k^{th} pole generated by B2P model, which is expressed as

$$G_k(d_{P,k}) = A_{ref,P} - 10n_k \log_{10}(d_{P,k}/d_{ref,P}) + S_P(d_{P,k}), \quad (8)$$

where $d_{P,k}$ is the distance between the BS and the k^{th} pole, $A_{ref,P}$ is the power gain at a reference distance $d_{ref,P}$, n_k is the path loss exponent, and $S_P(d_{P,k})$ is the large scale fading for the k^{th} pole, which is also modeled as a dynamic process with correlated characteristics. Based on the regression analysis we choose an exponential autocorrelation function [10],

$$r_P(\Delta d) = \sigma_P^2 e^{-\frac{\ln 2}{d_P}(\Delta d)}, \quad (9)$$

where d_P is the de-correlation distance and σ_P^2 is the variance of the lognormal fading.

As depicted in Fig. 1, the rail is regarded as the X-axis and the positive direction is the same as the train moving direction. The vertical distance between the pole and rail is 1.5 m. x_k is the projection of the k^{th} pole in the axis, $x(t)$ is the position of RX at time t, and the distance in P2R model is defined as $d_k(t) = x_k - x(t)$. Hence, $A_{P,0}(d_k(t))$ is the scattering factor modeled as

$$A_{P,0} = \begin{cases} -10n_{p,1}\log_{10}(d_k(t)/d_b), & d_b < d_k(t) \leqslant d_m \\ -n_{p,2}d_k(t) + \beta, & d_l \leqslant d_k(t) \leqslant d_b, \end{cases} \quad (10)$$

where d_m and d_l are the effective ranges as the poles mainly affect the RX in the vicinity of them, d_b is the distance between the peak position and the projection of the pole. $n_{p,i}$ are the estimated values of path loss exponents, and $\beta = n_{p,2}d_b$.

Fig. 5 depicts the normalized gain for all the poles in the measured region, and the red solid lines represent minimum root mean square error (RMSE) parameter estimates based on (10). When the RX comes close to the pole, the gain gradually increases with the decreasing propagation distance until a peak value, then decreases quite rapidly because of a large scattering angle, resulting that the receiver gets a weak scattering component. After the receiver has passed a pole, we would expect some diffracted paths. But when the receiver goes further and beyond certain effective range, the path gain becomes weak and is neglected in our model. Fig. 6 depicts the gain decay of the B2P model as a black curve and one sample generated by new PS model as a red curve, as seen the result matches well with the measurement data.

TABLE II
MODEL PARAMETERS

Parameters	**LOS**	**PS**
ϕ_X (rad)	$U(0, 2\pi)$	$U(0, 2\pi)$
$A_{ref,X}$ (dB)	-86.46	-92.67
n_L/n_k	3.88	3.00
$d_{ref,X}$ (m)	215.7	215.7
$d_{L,i}/d_P$ (m)	$56, 300, 330$	200
d_{p-p}, d_b, d_m, d_l (m)	/	$50, 5, 150, -10$
$n_{p,1}, n_{p,2}$	/	$1.50, -1.80$
$\sigma^2_{L,i}/\sigma^2_P$ (dB^2)	$0.9, 12.7, 3.0$	20.6

$X = \{LOS, PS\}$ and $i = \{1, 2, 3\}$.

IV. MODEL OUTLINE AND SIMULATION RESULTS

The general dynamic model consists of a LOS part and a PS part, and the channel impulse response is expressed as

$$h(t,\tau) = a_{LOS}(t)e^{i\frac{2\pi}{\lambda}c\cdot\tau_{LOS}(t)+i\phi_{LOS}}\delta(\tau-\tau_{LOS}(t)) + \sum_{k=1}^{K} a_{P,k}(t)e^{i\frac{2\pi}{\lambda}c\cdot\tau_{P,k}(t)+i\phi_{P,k}}\delta(\tau-\tau_{P,k}(t)), \quad (11)$$

where $a_X(t)$, $\tau_X(t)$ are the amplitudes, the delays of the respective MPCs at instant t. Furthermore, λ is the wave length and ϕ_X is the additive phase offset, assumed to be uniformly distributed without depending on t. The model parameters are listed in Table II.

The red curve in Fig. 7 shows one sample of the power gain generated by the new model with parameters as above. For comparison, we also include a sample generated with Lee's model [11], which contains a LOS path with a shadowing process, and scattering paths from a nearby circle, without the effect of poles along the rail. Obviously, our proposed model has a periodic characteristic and fits better with the measurement data. Fig. 8 shows one sample result of CDF plot of the root mean square (RMS) delay spread from the new model as a red line. The outcome of Lee's model depends largely on a choice of the scattering radius, and most of the values degrades the performance. Hence, it is better to model the channel according to the physical environments as our proposed model.

V. CONCLUSION

In this letter, we propose a dynamic channel model consisting of a LOS part and a pole scattering part for HSR communication based on measurements. The model focuses on the influence of overhead line poles along the rail, which block the LOS path periodically and act as static and periodic scatterers. The model behavior is demonstrated by simulations showing that the proposed model works well. The poles as special construction elements should be considered in channel modeling for HSR. Further studies should also consider the surrounding environment along the rail such as mountains, forests and large buildings.

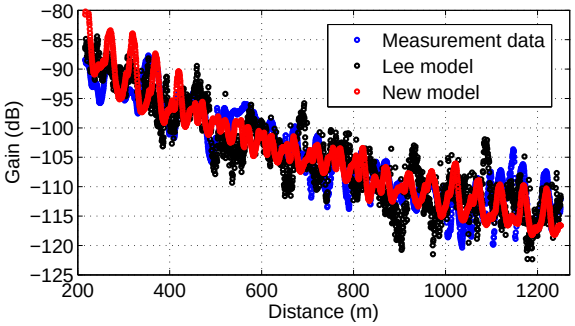

Fig. 7. Example plot of the gain along the rail.

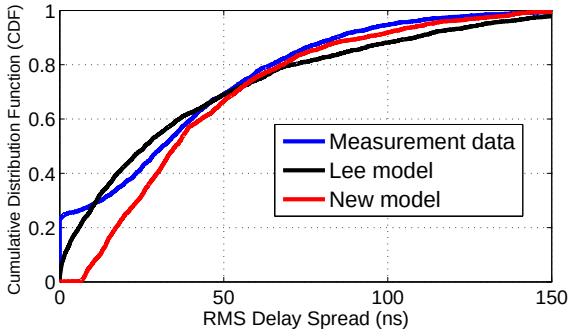

Fig. 8. Example plot of the RMS delay spread along the rail.

REFERENCES

[1] B. Chen et al., "A Geometry-Based Stochastic Channel Model for High-Speed Railway Cutting Scenarios," *IEEE Antennas and Wireless Propagation Letters*, vol. 14, pp. 851-854, 2015.

[2] J. Yang et al., "On the influence of mobility: Doppler spread and fading analysis in rapidly time-varying channels," *European Conference on Antennas and Propagation (EuCAP)*, 2016.

[3] B. Chen and Z. Zhong, "Geometry-Based Stochastic Modeling for MIMO Channel in High-Speed Mobile Scenario," *International Journal of Antennas and Propagation*, vol. 2012, 2012.

[4] K. Guan et al., "On the Influence of Scattering From Traffic Signs in Vehicle-to-X Communications," *IEEE Transactions on Vehicular Technology*, vol. 65, no. 8, pp. 5835-5849, Aug. 2016.

[5] T. Tie-Qiao, "A Dynamic Model for a Single Helicopter in the Low Airspace with Telegraph Poles and Electrical Wire," *Commun. Theor. Phys.*, vol. 56, no. 6, pp. 1149-1154, 2011.

[6] F. Luan, Y. Zhang, L. Xiao, C. Zhou, and S. Zhou, "Fading Characteristics of Wireless Channel on High-Speed Railway in Hilly Terrain Scenario," *International Journal of Antennas and Propagation*, vol. 2013, 2013.

[7] B. H. Fleury et al., "Channel Parameter Estimation in Mobile Radio Environments using the SAGE Algorithm," *IEEE Journal on Selected Areas in Communications*, vol. 17, no. 3, pp. 434-450, 1999.

[8] F. Luan et al., "Geometrical Cluster-Based Scatterer Detection Method with the Movement of Mobile Terminal," *IEEE Vehicular Technology Conference (VTC Spring)*, pp. 1-6, 2015.

[9] J. Karedal et al., "A Geometry-Based Stochastic MIMO Model for Vehicle-to-Vehicle Communications", *IEEE Trans. Wireless Communication*, vol. 8, no. 7, pp. 3646-3657, 2009.

[10] S. Gamini, "Multi-hop relay system evaluation methodology (Channel model and performance metrics)", *IEEE802.16j-06/013r3*, 2007.

[11] R. B. Ertel et al., "Overview of spatial channel models for antenna array communication systems," *IEEE Personal Communications*, vol. 5, no. 1, pp. 10-22, Feb. 1998.